

Selective Dimerization of a C2H2 Zinc Finger Subfamily

Aaron S. McCarty,¹ Gary Kleiger,^{1,2} David Eisenberg,^{1,2} and Stephen T. Smale^{1,3,*}

¹Howard Hughes Medical Institute
Molecular Biology Institute

²Department of Energy Center for Genomics
and Proteomics and

³Department of Microbiology, Immunology,
and Molecular Genetics
University of California, Los Angeles
Los Angeles, California 90095

Summary

The C2H2 zinc finger is the most prevalent protein motif in the mammalian proteome. Two C2H2 fingers in Ikaros are dedicated to homotypic interactions between family members. We show here that these fingers comprise a bona fide dimerization domain. Dimerization is highly selective, however, as homologous domains from the TRPS-1 and *Drosophila* Hunchback proteins support homodimerization, but not heterodimerization with Ikaros. Ikaros-Hunchback selectivity is determined by 11 residues concentrated within the α -helical regions typically involved in base recognition. Preferential homodimerization of one chimeric protein predicts a parallel dimer interface and establishes the feasibility of creating novel dimer specificities. These results demonstrate that the C2H2 motif provides a versatile platform for both sequence-specific protein-nucleic acid interactions and highly specific dimerization.

Introduction

The C2H2 zinc finger was first identified in transcription factor IIIA (TFIIIA) as a sequence-specific DNA binding motif that stabilizes its folds through the coordination of a central zinc ion (Miller et al., 1985; Wolfe et al., 2000). Although several other types of zinc-coordinating motifs have been identified (Mackay and Crossley, 1998; Schwabe and Klug, 1994), the C2H2 finger has emerged as the most prevalent protein motif in mammalian cells, with over 5000 encoded by the human genome (Lander et al., 2001; Venter et al., 2001). The prevalence of C2H2 fingers highlights their unusual versatility. This versatility is evident from the dramatic evolutionary expansion of C2H2 zinc finger proteins, from approximately 40 in *Saccharomyces cerevisiae* to over 800 in *Homo sapiens* (Lander et al., 2001; Venter et al., 2001). This expansion suggests that new genes with novel DNA binding specificities could be generated more readily by duplication and modification of C2H2 motifs than by modification of other types of DNA binding domains. The versatility of the C2H2 motif has been further demonstrated, and also exploited, by the successful engineering of C2H2

domains with novel DNA-sequence specificities (Pabo et al., 2001; Segal and Barbas, 2000, 2001).

The consensus sequence for C2H2 zinc fingers is (F/Y)-X-C-X₂₋₅-C-X₃-(F/Y)-X₅- ψ -X₂-H-X₃₋₅-H, where X is any amino acid and ψ is a hydrophobic residue (Wolfe et al., 2000). In addition to the cysteines and histidines that coordinate zinc, C2H2 fingers contain conserved hydrophobic residues that pack in the hydrophobic core. These conserved amino acids lead to the formation of the characteristic structure comprised of a two-stranded antiparallel β sheet and an α helix (see Figure 7A). Structures of several C2H2 domains bound to DNA have been solved by X-ray crystallography and NMR (Wolfe et al., 2000). The structures reveal that nucleotide base contacts are mediated primarily by residues near the N-terminal half of the α helix. The four residues most commonly involved in specific base recognition are at positions -1, 2, 3, and 6, relative to the beginning of the α helix.

Although most C2H2 fingers appear to contribute to protein-DNA and protein-RNA interactions, C2H2 fingers have also been implicated in protein-protein interactions (Mackay and Crossley, 1998). However, structural information has been obtained only for domains in which the contribution of the C2H2 finger to the protein-protein interaction is indirect. For example, dimerization of the RAG1 recombinase is mediated by a domain containing a RING finger and a C2H2 zinc finger (Bellon et al., 1997). In this domain, the C2H2 finger helps form a stable scaffold upon which the dimer interface is formed, but the finger does not directly participate in dimerization.

Ikaros is a protein expressed in hematopoietic cells that has been implicated in gene silencing and activation (Ernst et al., 1999; Georgopoulos, 2002). Four C2H2 fingers near the N terminus of Ikaros are involved in sequence-specific DNA binding (Hahm et al., 1994; Molnar and Georgopoulos, 1994). The C terminus contains two additional C2H2 zinc fingers that play no apparent role in the protein-DNA interaction (Hahm et al., 1994). Rather, previous studies using yeast two-hybrid screens and coimmunoprecipitation assays demonstrated that they are essential for self-interactions and for interactions with the corresponding zinc fingers of other Ikaros family members (Hahm et al., 1998; Sun et al., 1996; Honma et al., 1999; Perdomo et al., 2000). A protein fragment spanning the two zinc fingers was sufficient for the interaction, which was disrupted by mutations in the zinc-coordinating cysteines and histidines and by zinc displacement (Sun et al., 1996).

Although the C-terminal fingers of Ikaros did not directly contribute to protein-DNA interactions, they are critical for high-affinity DNA binding, which usually involves the recognition of tandem binding sites by two subunits of an Ikaros complex (Cobb et al., 2000; Molnar and Georgopoulos, 1994; Trinh et al., 2001). Homotypic interactions mediated by the C-terminal fingers are also necessary for the targeting of Ikaros to pericentromeric heterochromatin, which has been hypothesized to be important for the pericentromeric recruitment and heri-

*Correspondence: smale@mednet.ucla.edu

table silencing of Ikaros target genes (Brown et al., 1997, 1999; Cobb et al., 2000). Although the C-terminal fingers are involved in protein-protein interactions, rather than protein-DNA interactions, both fingers match perfectly the C2H2 consensus sequence, with the exception of a single missing F/Y in the second finger (Figure 1A). The absence of this F/Y does not explain its unusual function, however, as a hydrophobic residue is missing at this position in several DNA binding zinc fingers, including the first and third fingers of the DNA binding domain of Ikaros.

In this study, we have examined in greater depth the properties of this unusual C2H2 finger domain from the C terminus of murine Ikaros. We first established that the two C-terminal fingers comprise a bona fide dimerization domain that is necessary and sufficient for dimerization. We then demonstrated that homologous C2H2 domains from the murine TRPS 1 and *Drosophila* Hunchback proteins (Momeni et al., 2000; Tautz et al., 1987) also support dimerization. Dimerization was found to be highly selective, however, as the Ikaros domain was unable to form heterodimers with the TRPS 1 and Hunchback domains. Most interestingly, delineation of the amino acids responsible for Ikaros-Hunchback dimerization selectivity revealed that they reside largely within the same regions of the α helices that are responsible for base recognition in DNA binding zinc fingers. The selective homodimerization of one Ikaros-Hunchback chimera provides additional information about the dimer interface and establishes the feasibility of creating novel dimerization specificities.

Results

The C-Terminal Fingers of Ikaros Comprise a Bona Fide Dimerization Domain

To determine the stoichiometry of complexes formed by the C-terminal zinc fingers, gel filtration chromatography was performed with extracts from HEK 293 cells that overexpress Ikaros isoform I (IK I). IK I is a 32 kDa, naturally occurring isoform that lacks the DNA binding zinc fingers near the N terminus of the larger isoforms (Figure 1A). Immunoblot analysis of the gel filtration column fractions revealed a protein peak with an apparent molecular weight of 75 kDa (Figure 1B, top), most consistent with the predicted migration of an IK I dimer.

To determine whether the elution profile was dependent on the C-terminal fingers, two IK I mutants were tested. Mutant D18Q contains a substitution at aspartate 18 (Figure 1A), which is conserved in all Ikaros family members. This mutant eluted with an apparent molecular weight of 40 kDa (Figure 1B, middle), consistent with the migration of a monomer. Mutant m2/3 contains a complete replacement of the C-terminal fingers of IK I (fingers 5 and 6) with N-terminal DNA binding fingers 2 and 3 (Figure 1A). This mutant also eluted with an average molecular weight of 40 kDa (Figure 1B, bottom), demonstrating that only a subset of zinc fingers support dimerization.

To confirm the stoichiometry of the protein complexes, extracts containing IK I were incubated with the chemical crosslinking reagent, disuccinimidyl suberate (DSS). Crosslinked samples were analyzed by immunoblot. In the presence of high concentrations of DSS,

approximately 50% of the IK I protein migrated with a molecular weight of 67 kDa, consistent with the size of an IK I dimer (Figure 1D, lanes 19–21). A weak 85 kDa band was also observed, raising the possibility that IK I contains a domain that supports multimer formation, as previously suggested (Trinh et al., 2001). Crosslinked products were not observed with mutant D18Q (Figure 1D, lanes 4–6) or mutant m2/3 (data not shown), demonstrating that crosslinking is dependent on the intact C-terminal fingers.

To examine this interaction in greater detail, a smaller protein was prepared that contains only 79 amino acids from the N terminus of IK I (NTS) fused to a 64 amino acid region containing the C-terminal zinc fingers. A FLAG epitope tag was included at the N terminus. This 18 kDa protein, f-IkDZF, migrated with a molecular weight of 23 kDa (Figure 1D, lanes 1 and 16). Following crosslinking, most of the protein molecules migrated with a molecular weight of 40 kDa (Figure 1D, lanes 2, 3, 17, and 18), as expected for a protein dimer. Larger crosslinked products were not observed with this small protein, confirming that the C-terminal fingers represent a dimerization domain. We have named this 64 amino acid region the Dimerization Zinc Finger (DZF) domain.

To examine the stability of dimers formed via the Ikaros DZF, extracts containing IK I were mixed with extracts containing f-IkDZF. After incubation at room temperature for 1, 3, or 10 min, DSS was added, followed by incubation for an additional 7 min. The immunoblot results revealed the emergence of a band corresponding in size to heterodimers between IK I and f-IkDZF (Figure 1D, lanes 23–30). This band was relatively weak in the sample incubated for a total of 8 min (lanes 23 and 24). However, in the sample incubated for 17 min, the relative intensities of the bands corresponding to homodimers and heterodimers suggest that the exchange reaction had reached equilibrium (lanes 29 and 30). In a parallel experiment using the D18Q mutant in place of IK I, crosslinked products corresponding to f-IkDZF/D18Q heterodimers were much less abundant (Figure 1D, lanes 8–15), demonstrating that a functional DZF is important for the formation of f-IkDZF/IK I heterodimers. These results demonstrate that, although dimerization is efficient, dissociation and subunit exchange can occur quite rapidly. Efforts to quantify binding affinities and association and dissociation rates have been hampered by the challenge of expressing a functional DZF in *E. coli*.

As a routine assay for DZF-mediated dimerization, the f-IkDZF protein or a variant of this protein was coexpressed in HEK 293 cells with untagged IK I or an IK I variant (Figure 1C). Dimerization was then monitored by immunoprecipitation with the FLAG M2 monoclonal antibody, followed by extensive washing and immunoblot analysis using Ikaros antibodies that recognize the common NTS (see Figure 1A). Using this assay, f-IkDZF supported efficient coimmunoprecipitation of untagged IK I (Figure 1C, lane 3). The high efficiency of coimmunoprecipitation confirmed that most protein molecules exist as dimers. IK I did not precipitate from extracts lacking the f-IkDZF protein and was not observed in either the extract or immunoprecipitation pellet when the IK I expression plasmid was omitted from the transfection (Figure 1C, lanes 1 and 2). IK I coimmunoprecipitation was not dependent on nucleic acids, as

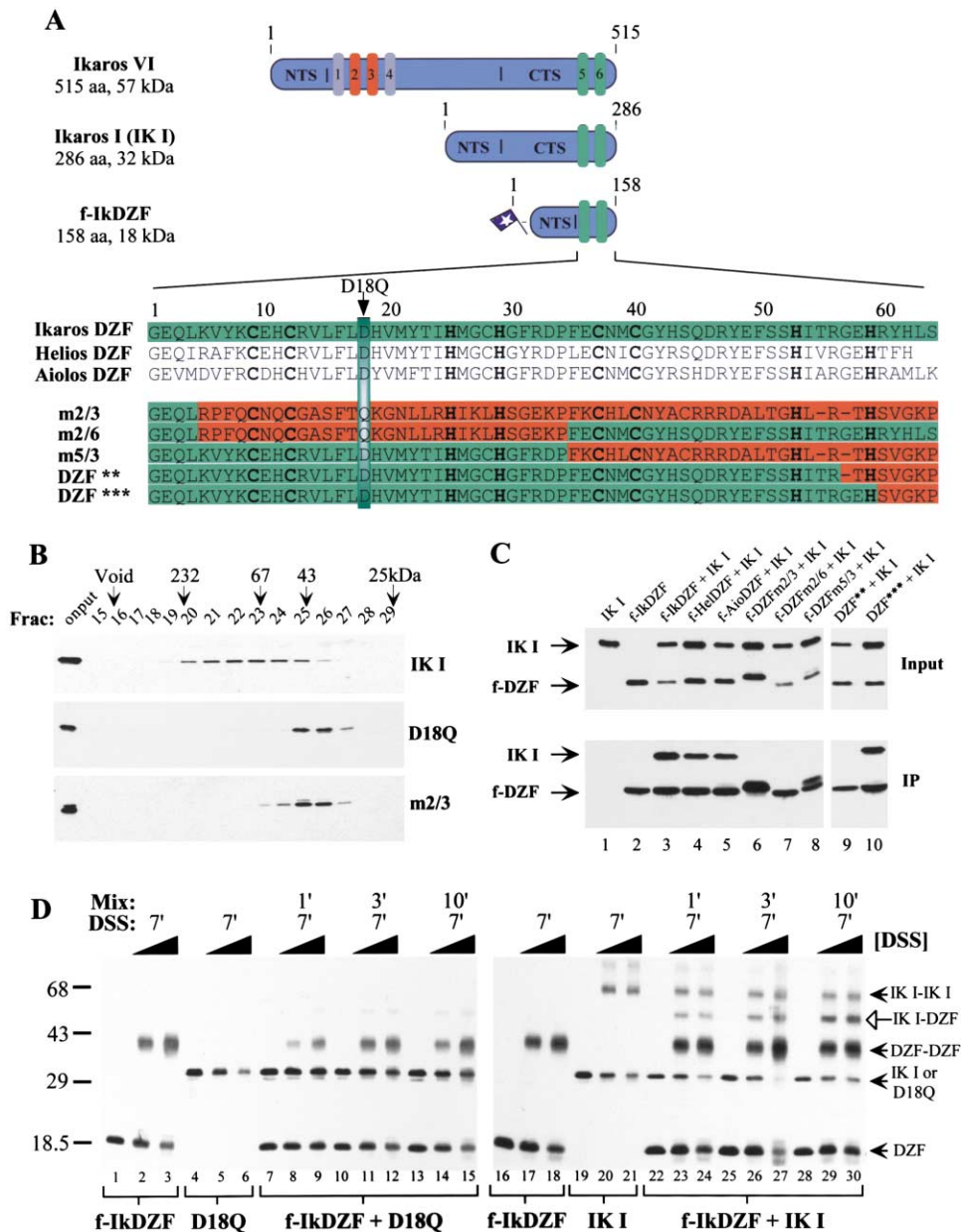


Figure 1. Dimerization of the Ikaros C-Terminal Zinc Fingers

(A) Full-length Ikaros isoform VI contains four N-terminal C2H2 zinc fingers that mediate DNA binding and two C-terminal C2H2 fingers that support interactions between family members. IK I is a naturally occurring isoform that arises through alternative pre-mRNA splicing. f-IkDZF contains a FLAG epitope tag, the Ikaros N-terminal sequence (NTS), and 64 residues encompassing the C-terminal fingers. The sequences of the C-terminal zinc fingers of murine Ikaros, Helios, and Aiolos, and of five Ikaros mutants, are shown. Mutant amino acids derived from N-terminal fingers 2 and 3 are in red.

(B) Extracts of HEK 293 cells overexpressing wt or mutant IK I proteins were analyzed by gel filtration chromatography.

(C) Interactions between overtagged and FLAG-tagged proteins were analyzed using a coimmunoprecipitation assay. Extracts were from 293 cells cotransfected with expression plasmids for untagged proteins in the context of IK I and smaller FLAG-tagged proteins. Extracts were analyzed prior to immunoprecipitation (top) and following immunoprecipitation with the FLAG M2 monoclonal antibody (bottom). Proteins were visualized by immunoblot using antibodies directed against the Ikaros NTS. Proteins containing finger 3 migrate more slowly through SDS protein gels (lanes 6 and 8).

(D) Chemical crosslinking of proteins within HEK 293 extracts was performed with DSS. In the mixing experiments, extracts from cells transfected with f-IkDZF were mixed for variable times (1–10 min) with extracts from cells transfected with either D18Q (lanes 7–15) or IK I (lanes 22–30). Crosslinking was then carried out for 7 min, followed by immunoblot analysis.

the results were unaltered in the presence of ethidium bromide, DNase I, and RNase A (data not shown).

To monitor the specificity of dimerization, the closely related DZF domains from Ikaros family members Aiolos

and Helios (Figure 1A) were substituted for the Ikaros DZF in the context of the FLAG-tagged protein, creating f-AioDZF and f-HelDZF. These proteins supported efficient coimmunoprecipitation of IK I (Figure 1C, lanes 4

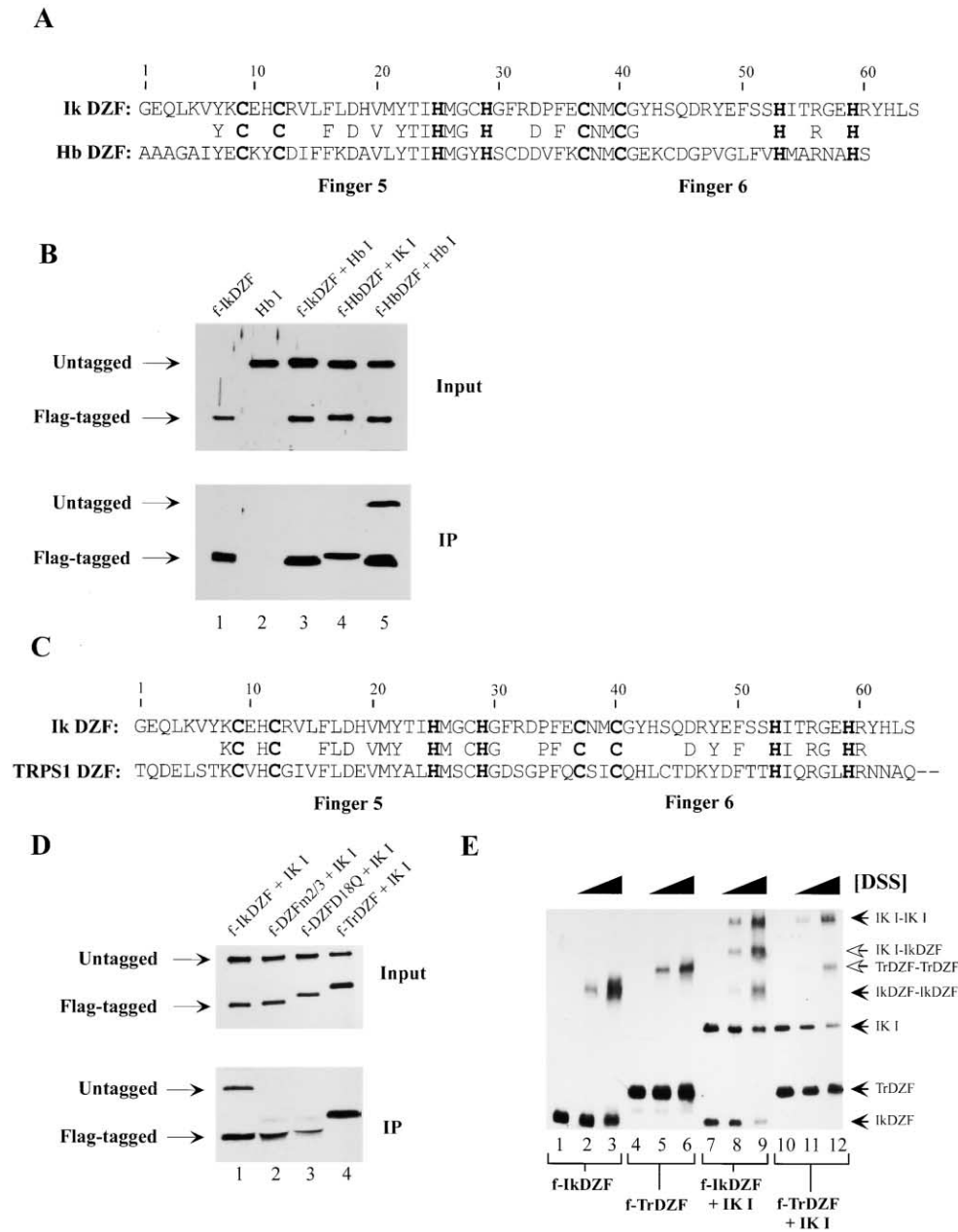


Figure 2. Selective Interactions Mediated by DZF Domains

- (A) DZF sequences from the murine Ikaros and *D. melanogaster* Hunchback proteins are aligned.
 (B) Interactions between untagged proteins in the context of IK I and smaller FLAG-tagged proteins were analyzed using the coimmunoprecipitation assay.
 (C) DZF sequences from the murine Ikaros and human TRPS 1 proteins are aligned.
 (D) Interactions between untagged proteins in the context of IK I and smaller FLAG-tagged proteins were analyzed using the coimmunoprecipitation assay.
 (E) Dimerization of the Ikaros and TRPS 1 DZF domains was analyzed using the chemical crosslinking assay.

and 5), consistent with previous reports (Hahm et al., 1998; Sun et al., 1996). In contrast, coimmunoprecipitation of IK I was not observed when DNA binding fingers 2 and 3 were introduced into the FLAG-tagged protein in place of the DZF (f-DZFm2/3, Figure 1C, lane 6). Coimmunoprecipitation was also undetectable when DNA binding finger 2 was substituted for DZF finger 5 (f-DZFm2/6) and when DNA binding finger 3 was substituted for DZF finger 6 (f-DZFm5/3, Figure 1C, lanes 7 and 8). (Note

that all proteins containing finger 3 migrate with slower mobility for reasons that remain unknown.) The specificity of the interaction was further confirmed by the absence of coimmunoprecipitation when only 8 amino acids at the C terminus of DZF finger 6 were replaced by the corresponding amino acids from DNA binding finger 3 (f-DZF**, lane 9). The interaction was retained when the substitution was restricted to 5 amino acids (f-DZF***, lane 10).

Highly Selective Dimerization Mediated by the DZF Domain

The zinc finger organization found in mammalian Ikaros proteins also exists within the *Drosophila* gap segmentation protein Hunchback (Tautz et al., 1987). The C-terminal fingers of Ikaros and Hunchback exhibit considerable sequence homology (Figure 2A), suggesting that the Hunchback fingers may support dimer formation. To examine this possibility, the Hunchback C-terminal fingers were substituted for the Ikaros DZF in the context of both the epitope-tagged protein (f-HbDZF) and untagged IK I (Hb I). Hb I efficiently coimmunoprecipitated with f-HbDZF (Figure 2B, lane 5), confirming that Hunchback C-terminal fingers contain a functional DZF domain. Interestingly, Hb I did not coimmunoprecipitate with f-IkDZF, and IK I did not coimmunoprecipitate with f-HbDZF (Figure 2B, lanes 3 and 4). These results demonstrate that DZF-mediated dimerization is selective. This surprising degree of selectivity was equally apparent in chemical crosslinking experiments (see Figure 6 below).

Recently, the human TRPS 1 protein, which is responsible for tricho-rhino-phalangeal syndrome, was found to contain a C-terminal domain with homology to the Ikaros DZF (Momeni et al., 2000). When this domain from murine TRPS 1 (Figure 2C) was expressed in the context of a small, FLAG-tagged protein, it could not coimmunoprecipitate IK I (Figure 2D, lane 4). Chemical crosslinking experiments confirmed that this small protein, f-TrDZF, can form homodimers, but not heterodimers with IK I (Figure 2E). When f-TrDZF was expressed by itself and incubated with DSS, a band corresponding in size to an f-TrDZF homodimer was observed (Figure 2E, lanes 5 and 6). This same f-TrDZF homodimer band, along with a band corresponding to an IK I homodimer, was observed when f-TrDZF and IK I were coexpressed and incubated with DSS (Figure 2E, lanes 11 and 12). However, in these same samples, a band corresponding in size to an IK I-TrDZF heterodimer was not detected. In parallel samples, coexpression of IK I and f-IkDZF yielded cross-linked products corresponding in size to both homodimers and heterodimers (Figure 2E, lanes 8 and 9).

Determinants of Dimerization Selectivity Identified by Chimeric Protein Analyses

To identify the amino acid determinants of selective dimerization, the Ikaros and Hunchback DZF sequences were first compared (Figure 2A). This comparison revealed striking similarities and differences. Within the 60 amino acid region, 23 of the amino acids (38%) are identical, consistent with the conserved functions of the domains. The atypical length of the spacer between the final two histidines (5 residues) is also conserved. Despite the high degree of identity, five positions contain charge reversals, ten positions vary between charged and nonpolar residues, and seven positions vary between polar and nonpolar residues. These three categories represent 37% of the DZF amino acids, making it difficult to predict which residues are responsible for dimerization selectivity. Comparison of the Ikaros and TRPS 1 DZF sequences, or the Hunchback and TRPS 1 sequences, revealed similar degrees of identity and divergence.

Because of the high degree of divergence, a system-

atic approach was necessary to identify the determinants of selective dimerization. As a starting point, two series of Ikaros-Hunchback DZF chimeras were generated in the context of untagged IK I (Figures 3A and 4A). These chimeras were expressed in HEK 293 cells along with either f-HbDZF or f-IkDZF. Protein-protein interactions were monitored using the coimmunoprecipitation assay.

The first series of chimeras contains decreasing amounts of the Hunchback DZF N terminus fused to increasing amounts of the Ikaros DZF C terminus (Hb-IK1 to Hb-IK6, Figure 3A). An efficient interaction with f-HbDZF was retained when Ikaros amino acids 53–64 were included in the chimeric protein (Hb-IK2, Figure 3B, lane 3), but not when amino acids 47–64 were included (Hb-IK3, Figure 3B, lane 4). These results suggest that at least 1 residue between amino acids 47 and 52 is required for selective homodimerization of the Hunchback DZF, but that amino acids 53–64 are not involved in selectivity.

The second series of chimeric proteins was used to define the amino acids at the N terminus of the Hunchback DZF that are required for selective dimerization. This series contains decreasing amounts of the Ikaros DZF N terminus fused to increasing amounts of the Hunchback DZF C terminus (Ik-Hb1 to Ik-Hb6, Figure 4A). An efficient interaction with the f-HbDZF protein was observed when Ikaros amino acids 1–14 were included in the chimeric protein (Ik-Hb5, Figure 4B, lane 5), but the interaction was lost when Ikaros amino acids 1–27 were included (Ik-Hb4, Figure 4B, lane 6). These results demonstrate that at least 1 residue between amino acids 15 and 27 is required for selectivity and that amino acids 1–14 are not involved. Thus, the residues involved in selective dimerization of the Hunchback DZF are located between amino acids 15 and 52 (summarized in Figure 5D).

The two sets of chimeric proteins were then used to define the region required for dimerization with the Ikaros DZF. Using the Hb-Ik series (Figure 3A), an efficient interaction with f-IkDZF was observed when the chimeric protein included Hunchback amino acids 1–27 (Hb-Ik6, Figure 3C, lane 7). However, an interaction was not observed when Hunchback amino acids 1–31 were included (Hb-Ik5, Figure 3C, lane 6). Using the Ik-Hb series (Figure 4A), an efficient interaction with the f-IkDZF protein was observed when the chimeric protein included Hunchback amino acids 52–60 (Ik-Hb1, Figure 4C, lane 8). Inefficient coimmunoprecipitation was observed when the chimeric protein included Hunchback amino acids 34–60 (Ik-Hb2, Figure 4C, lane 7), and no coimmunoprecipitation was observed when Hunchback amino acids 32–60 were included (Ik-Hb3, Figure 4C, lane 6). These results suggest that the residues contributing to selective dimerization of the Ikaros DZF are located between amino acids 28 and 51 (Figure 5D).

Contributions of Specific Amino Acids to Dimerization Selectivity

To define more precisely the amino acids involved in selective dimerization of the Ikaros DZF, all of the amino acids that differ between the Ikaros and Hunchback DZFs (between amino acids 1 and 59) were replaced, either individually or in pairs. To create these substitu-

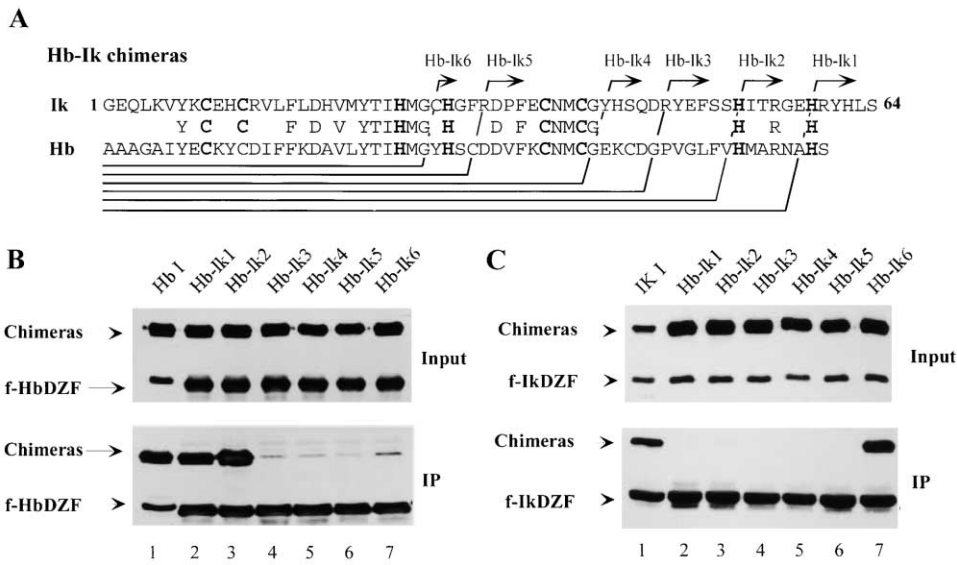


Figure 3. Chimeric Protein Analysis to Delineate the DZF Regions that Contribute to Selective Dimerization (A) The Hunchback and Ikaros sequences included in each Hb-Ik chimera are shown. (B) Interactions between Hb-Ik chimeras and f-HbDZF were assessed using the coimmunoprecipitation assay. (C) Interactions between Hb-Ik chimeras and f-IkDZF were assessed using the coimmunoprecipitation assay.

tions, Hunchback DZF amino acids were inserted at the corresponding positions of the Ikaros DZF in the context of the f-IkDZF protein.

The interactions between the mutant f-IkDZF proteins and wild-type IK 1 were first monitored using the coimmunoprecipitation assay. In this assay, coimmunoprecipitation of IK 1 was strongly reduced with 9 of the 23 mutant proteins (Figure 5A, lanes 9, 11, 12, 15, and

18–22). A combined total of 13 residues were altered in these nine mutants.

To confirm that these mutations disrupt dimerization, the mutant proteins were tested in the chemical cross-linking assay. This assay is thought to be less stringent than the coimmunoprecipitation assay because extensive high-salt washes are not involved. As shown in Figure 5B, mutant DZF-DZF homodimers were unde-

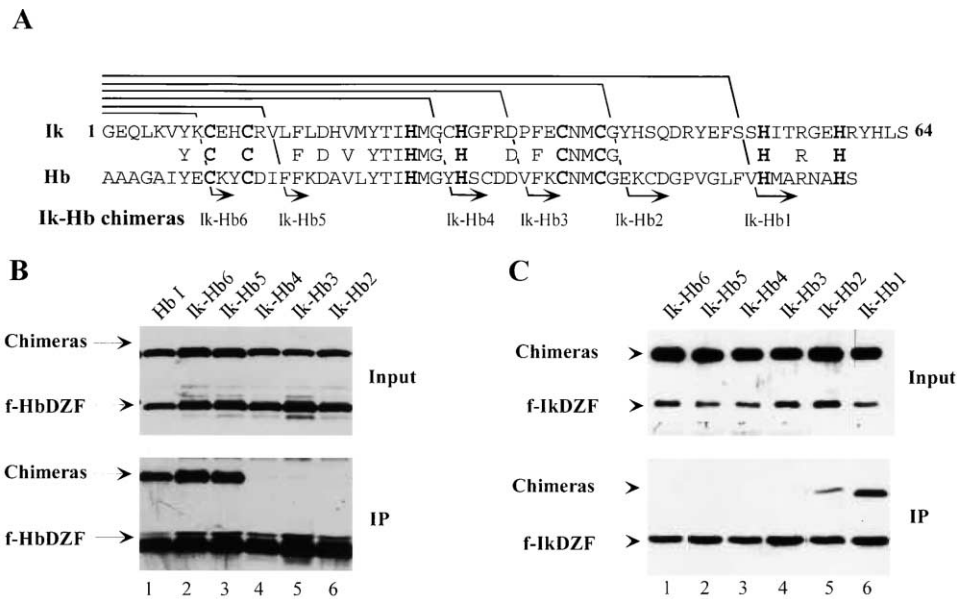


Figure 4. Chimeric Protein Analysis to Delineate the DZF Regions that Contribute to Selective Dimerization (A) The Ikaros and Hunchback sequences included in each Ik-Hb chimera are shown. (B) Interactions between Ik-Hb chimeras and f-HbDZF were assessed using the coimmunoprecipitation assay. (C) Interactions between Ik-Hb chimeras and f-IkDZF were assessed using the coimmunoprecipitation assay.

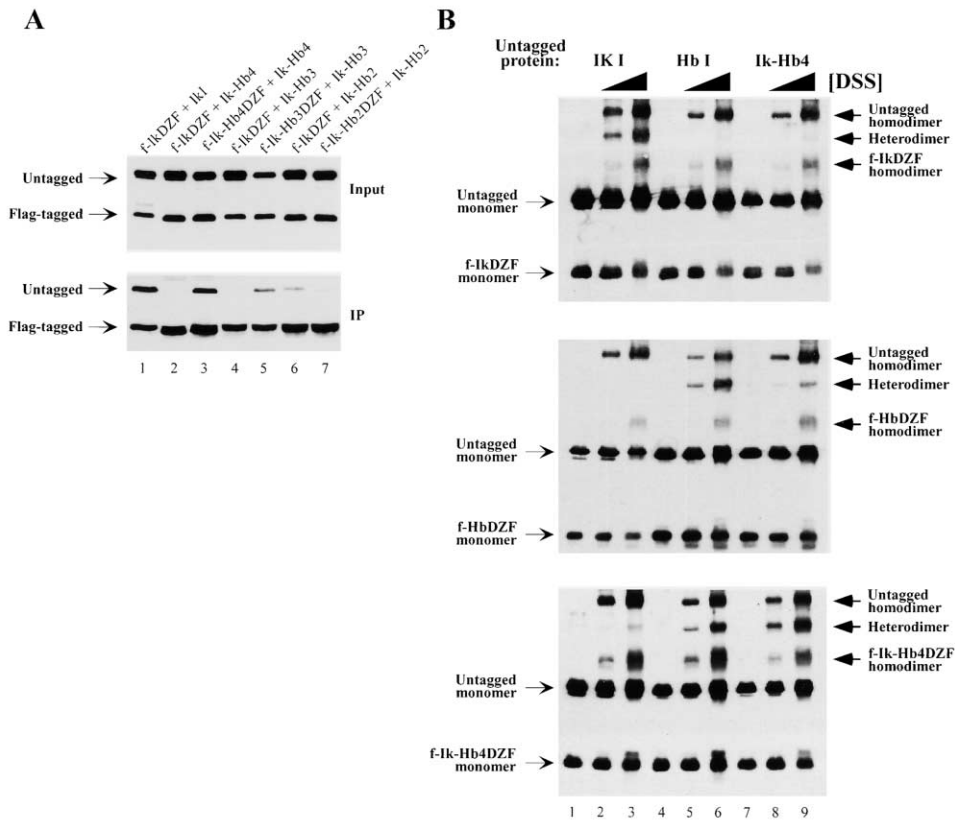


Figure 6. Selective Dimerization of Ikaros-Hunchback Chimeras

(A) Self-association of Ik-Hb4, Ik-Hb3, and Ik-Hb2 was assessed using the coimmunoprecipitation assay. The chimeric DZFs were expressed in the context of both the larger untagged protein and the smaller FLAG-tagged protein.

(B) Self-association of Ik-Hb4 and association with the Ik DZF and Hb DZF were assessed using the crosslinking assay. Multimeric species at the top were omitted for simplicity (see Figure 1D, lanes 20 and 21).

heterodimerization were observed with the remaining two mutants (lanes 18 and 30). These results demonstrate that a maximum of 10 residues contribute to selective Ikaros dimerization when the interaction is monitored using the crosslinking assay (residues 17, 21, 28, 34, and 46–51). An additional 3 residues (residues 44, 45, and 52) are required for Ikaros dimerization to withstand the stringent washes employed in the coimmunoprecipitation assay.

Because 2 residues were altered in four of the critical mutants, it was important to determine whether one or both residues in each mutant are required for dimerization. Using the chemical crosslinking assay, single substitutions of R47 and F50 disrupted dimerization (Figure 5C, lanes 6 and 15). Mutations at Y48 and E49 slightly reduced but did not eliminate dimerization (Figure 5C, lanes 9 and 12); these single residue substitutions were less detrimental than the mutation that alters both residues simultaneously (Figure 5B, lane 27). In contrast, mutations at D46 and S51 did not significantly affect dimerization (Figure 5C, lanes 3 and 18). Similar results were obtained in the coimmunoprecipitation assay. However, in this assay, Y48 and E49 were both essential for dimerization, as coimmunoprecipitation of IK I was not observed (data not shown). The results of the mutant analysis are summarized in Figure 5D and are discussed below (see Discussion).

Preferential Homodimerization of an Ikaros-Hunchback DZF Chimera

The identification of two distinct DZF specificities raises the question of whether novel specificities can be created. To address this question, we focused on the three chimeric proteins that were unable to coimmunoprecipitate efficiently with either f-IkDZF or f-HbDZF (Ik-Hb4, Ik-Hb3, and Ik-Hb2). Coexpression of Ik-Hb4 in the context of both the tagged and untagged proteins revealed its capacity to form homodimers (Figure 6A, lane 3). Less efficient homodimerization was detected with Ik-Hb3 (Figure 6A, lane 5), while Ik-Hb2 was unable to homodimerize (Figure 6A, lane 7).

The Ik-Hb4 results were confirmed using the less stringent chemical crosslinking assay. Crosslinking was performed with extracts from HEK 293 cells in which small and large DZF-containing proteins were overexpressed simultaneously. f-IkDZF/IK I dimers were readily apparent (Figure 6B, lanes 1–3, top panel), but f-IkDZF/Hb I and f-IkDZF/ik-Hb4 heterodimers were undetectable (lanes 4–9, top panel). Similarly, f-HbDZF/Hb I dimers were apparent (lanes 4–6, center panel), but f-HbDZF/IK I heterodimers were absent (lanes 1–3, center panel). An f-HbDZF/IK-Hb4 dimer was detectable (lanes 7–9, center panel), but was less abundant than the f-HbDZF or Ik-Hb4 homodimers observed in the same reactions. Detection of f-HbDZF/ik-Hb4 heterodimers in this assay,

but not in the coimmunoprecipitation assay, is presumably due to the reduced stringency of this assay. Finally, abundant f-Ik-Hb4/Ik-Hb4 dimers (lanes 7–9, bottom panel) and slightly less abundant f-Ik-Hb4/Hb I dimers (lanes 4–6, bottom panel) were present, but f-Ik-Hb4/Ik I dimers were undetectable (lanes 1–3, bottom panel).

Taken together, the coimmunoprecipitation and cross-linking results demonstrate that IK-Hb4 preferentially homodimerizes. Although an interaction between this chimera and the Hunchback DZF was observed in the crosslinking experiments, the absence of coimmunoprecipitation in Figure 4B suggests that this heterodimer is relatively unstable. Thus, these results establish the principle that novel DZF homodimer preferences can be created. Because the Ik-Hb4 chimera combines the N-terminal DZF finger from Ikaros with the C-terminal DZF finger from Hunchback, the preferential homodimerization of this protein provides strong support for a parallel interaction between the dimer subunits.

Discussion

This study provides insight into a C2H2 zinc finger domain that is dedicated to homodimerization and heterodimerization with closely related family members. It is well established that protein-protein interactions can be supported by zinc binding motifs that are distinct, both structurally and at the amino acid sequence level, from the more prevalent C2H2 zinc finger (Bellon et al., 1997; Fox et al., 1998; Liew et al., 2000; Mackay and Crossley, 1998). In addition, a few C2H2 DNA binding motifs have been shown to interact with other proteins (Lee et al., 1993; Payre et al., 1997; Zhou et al., 1995). These interactions have not been examined in detail but appear to involve regions of the zinc fingers that are distinct from the protein-DNA interface. The DZF domain described here is unique in three respects. First, the DZF domain supports efficient homotypic interactions rather than interactions with other types of domains. Second, dimerization is highly selective, as the Ikaros, Hunchback, and TRPS 1 domains can form homodimers, but not heterodimers, even when dimerization is monitored using the nonstringent crosslinking assay. Third, dimerization selectivity relies primarily on amino acids near the N terminus of the putative α helix, the same region involved in selective base recognition in DNA binding zinc fingers (Wolfe et al., 2000).

Using a homology model of the Ikaros DZF, we note that 7 of the 8 residues identified in this manuscript as important for selective dimerization cluster on the surface of the model (Figures 7B and 7C, red). We infer that these patches are likely to represent the dimer interface. The clusters correspond primarily to the α helices of both zinc finger domains. Within the first finger, the clustering of the 3 critical residues, L17, M21, and C28 (red residue to the right of L17 in Figure 7B), was expected on the basis of the 7 residue spacing between M21 and C28 on the α helix, and the 4 residue spacing between M21 and L17 (which is at the end of the second β strand). Because the orientation of the α helix is constrained by the conserved hydrophobic residue, Y22, which packs in the hydrophobic core, there is a high probability that these critical residues will be exposed in the DZF structure. For reference, a ribbon diagram of

a typical C2H2 finger motif is shown in Figure 7A and is oriented similarly to finger 1 in Figure 7B.

In the second finger, the 4 residues that are most important for selective dimerization, R47, Y48, E49, and F50, are adjacent to one another on the α helix. A hydrophobic residue that packs in the core is expected at the position occupied by F50. Therefore, this residue is almost certainly at the core and does not directly contribute to the dimer interface. Instead, F50 is likely to make an important contribution to the structure of the finger. Interestingly, this residue cannot be replaced by the leucine found at the same position in the Hunchback DZF. This observation suggests that the structures of the hydrophobic cores of the Ikaros and Hunchback DZFs differ, which may be important for selectivity.

Residues R47, Y48, and E49 are likely to be important constituents of the dimer interface. Because the hydrophobic cores of C2H2 motifs are highly compact, all three of these residues are likely to be exposed. However, the precise orientations of the amino acid side chains cannot be determined in the absence of an experimentally defined structure. The presence of arginine, tyrosine, and glutamate residues at the Ikaros dimerization interface (R47, Y48, and E49) suggests that a combination of salt bridges, hydrogen bonds, and hydrophobic interactions stabilize the dimer. Equivalent positions of the Hunchback DZF sequence contain hydrophobic residues, suggesting that stabilization of the Hunchback dimerization interface may be more dependent on van der Waals interactions.

Although 7 of the 8 critical residues are located in the clusters described above, the eighth residue, P34 (Figures 7B and 7C; green), is located in the linker region between the two zinc finger domains. A proline residue is expected to reduce flexibility of the protein main chain. Therefore, the requirement for this residue for the formation of Ikaros dimers suggests that the relative orientations of the two finger domains may contribute to selectivity.

The 3 residues that were less important for dimerization (because mutations disrupted dimerization only in the stringent coimmunoprecipitation assay; S44, Q45, S53) cluster adjacent to the patches formed by the 7 critical residues (Figures 7B and 7C; orange). Finally, a subset of the residues that are conserved among all of the DZFs that have been characterized (in Ikaros, Aiolos, Helios, Hunchback, and TRPS1) are in close proximity to the two patches (Figures 7D and 7E; blue). D18, which was shown to be essential for dimerization in Figure 1, is located at a particularly prominent position of the finger 1 cluster (Figure 7D).

It is interesting to note that the two key clusters correspond to the regions that typically contact specific bases in DNA binding zinc fingers. The residues that most frequently contact bases are at positions -1 , 2 , 3 , and 6 (Figure 5D, circled), where position $+1$ corresponds to the first residue on the helix (Wolfe et al., 2000). In this region of the first DZF finger, the critical residues L17 and M21 correspond to positions -2 and $+3$. The third critical residue, C28, is at position 10 , which contributes an essential base contact in TFIIIA (Wolfe et al., 2000; Wuttke et al., 1997). Within the second DZF finger, the 7 residues that contributed to selective dimerization lie between positions -3 and $+6$. These

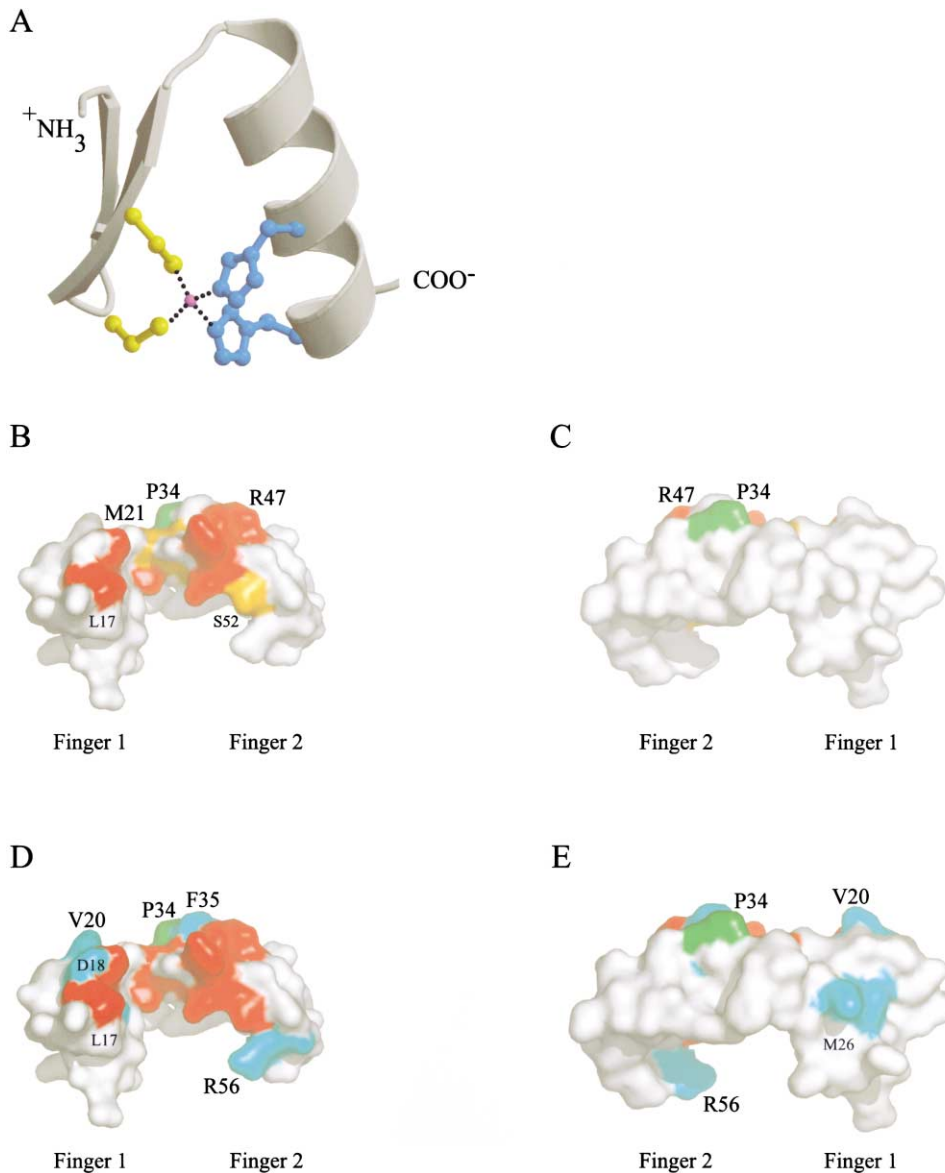


Figure 7. Homology Model of the Ikaros DZF Domain

(A) Ribbon diagram of a typical zinc finger domain from a protein engineered to bind a TATA box (Protein Data Bank code 1G2D [Wolfe et al., 2001]). The finger contains the conserved cysteine (gold) and histidine (blue) residues that coordinate a zinc ion within the core. The diagram is oriented similarly to DZF finger 1 in the following models.

(B) Surface representation of the Ikaros DZF homology model. The N-terminal finger, finger 1, is on the left; the C-terminal finger, finger 2, is on the right. The residues that, when mutated, perturb dimerization in both the crosslinking and coimmunoprecipitation assays are colored red (L17, M21, C28, R47, Y48, E49, and F50). Mutation of P34 (green) in the linker region also disrupts dimerization in both assays. The 3 residues that, when mutated, perturb dimerization only in the stringent coimmunoprecipitation assay are colored orange (S44, Q45, and S52). A subset of these colored residues are labeled.

(C) 180° rotation about the vertical axis of the homology model shown in (B). Mutation of the residues on this side of the molecule to the Hunchback sequence does not affect homodimerization, supporting the notion that the binding interface is on the other side of the molecule.

(D) Identical to (B), except residues in Ikaros that are identical in Hunchback, TRPS1, Aiolos, and Helios are colored blue (F16, D18, V20, Y22, M26, F35, and R56). In addition, the 3 residues shown in orange in part (B) are colored red.

(E) 180° rotation about the vertical axis of the model in (D). These figures were generated using the program PYMOL (<http://www.pymol.org>).

observations demonstrate that similar structural elements are involved in selective dimerization and in selective protein-DNA interactions.

Previous studies demonstrated that C2H2 zinc fingers can be manipulated more easily than other DNA binding motifs to generate novel DNA-sequence specificities

(Isalan et al., 2001; Pabo et al., 2001; Segal and Barbas, 2000, 2001). The preferential homodimerization of one of the Ikaros-Hunchback chimeras suggests that it may be possible to perform similar types of manipulations to generate novel dimerization specificities. Previous examples in which the specificity of a dimerization motif

has been altered include the conversion of homodimer and heterodimer preferences of leucine zippers (O'Shea et al., 1992; Sellers and Struhl, 1989).

Because of the importance of protein dimerization for cellular processes, strategies for promoting dimerization in a cell are of considerable interest (Klemm et al., 1998). The ability to create novel dimerization specificities is already benefiting our studies of Ikaros, as fully functional Ikaros family members that cannot dimerize with endogenous Ikaros proteins can now be engineered and expressed in lymphocytes. In previous attempts to avoid dimerization with endogenous Ikaros proteins, the C-terminal zinc fingers were replaced by a leucine zipper from a *Arabidopsis* GBF protein (Cobb et al., 2000). Although this leucine zipper does not appear to interact with mammalian leucine zipper proteins, it is difficult to exclude this possibility. Furthermore, the leucine zipper has greater potential to disrupt the functions of Ikaros proteins than more subtle mutations that alter the specificity of the DZF. Altered specificity DZF domains may be useful for promoting the selective dimerization of other ectopically expressed proteins. Although highly speculative at this time, it is also conceivable that it will be possible to design DZF domains that support selective interactions with any protein surface, which would parallel most closely the creation of C2H2 zinc fingers capable of binding any DNA sequence (Isalan et al., 2001; Pabo et al., 2001).

Finally, it is noteworthy that a dramatic expansion of the C2H2 zinc finger family has been documented during eukaryotic evolution (Lander et al., 2001; Venter et al., 2001). The evidence that the C2H2 zinc finger can use similar structural elements both for sequence-specific DNA binding and for selective dimerization confirms the unusual versatility of the motif and may explain, in part, the rapid expansion of the C2H2 family. It is noteworthy that all of the proteins that contain well-documented DZF domains contain other C2H2 zinc finger domains that support DNA binding. One can speculate that the DZF originally emerged in a Hunchback ancestor by duplication of the C2H2 DNA binding zinc fingers, followed by mutation and selection to create a dimer interface. This strategy for adding a dimerization domain to the ancient protein may have been easier to accomplish than the transposition of a dimerization domain-encoding exon from another gene.

Experimental Procedures

Plasmids and Transfections

HEK 293T cells were transfected by the calcium phosphate method (Ausubel, 1995), using 1 or 2 μ g DNA for expression of tagged and untagged proteins, respectively. Cells were harvested after 48 hr as described (Hahm et al., 1994, 1998), except the cytoplasmic fractions were retained for analysis. Plasmids were prepared by standard PCR methods in pcDNA3 (Invitrogen). Briefly, the desired coding regions were amplified from mRNA or cDNA clones using 5' and 3' oligonucleotides that were homologous to 21 nucleotides of gene sequence. 5' oligonucleotides contained a HindIII or KpnI recognition site followed by a Kozak sequence. For expression of tagged proteins, the p690 vector was generated by ligating a FLAG-encoding (DYKDDDDK) duplex oligonucleotide into pcDNA3 (HindIII and KpnI sites). Expression plasmids for Ikaros-Hunchback chimeras were created by PCR SOEING (Horton, 1995). Expression plasmids for substitution mutants were prepared using the QuickChange

method (Stratagene). All plasmids were confirmed by DNA sequencing.

Gel Filtration Chromatography

Gel filtration chromatography was performed with a Superose 12 HR 10/30 column (Pharmacia) equilibrated with Buffer H₆₀ (20 mM HEPES, pH 7.9, 1.5 mM MgCl₂, 60 mM KCl). The column was controlled by a Pharmacia LCC 500 Plus Control Module attached to Pharmacia P-500 pumps and was subjected to constant flow at a rate of 0.5 ml/min. Protein Sizing Standards (Pharmacia) were used to calibrate elution volumes. After calibration, 200 μ l (~800 μ g) of cytoplasmic lysate was injected and run under identical conditions. 400 μ l fractions were collected, and 10–30 μ l aliquots were separated by 12% SDS-PAGE. Proteins were visualized by immunoblot analysis using Ikaros antibodies (Hahm et al., 1994, 1998).

Coimmunoprecipitation Assays

Cytoplasmic extracts were clarified by microcentrifugation for 2 min prior to use. In a typical experiment, 10 μ l of lysate were diluted to a volume of 200 μ l with cold RIPA buffer (150 mM NaCl, 50 mM Tris, pH 7.5, 0.1% SDS, 0.025% sodium deoxycholate, 1% NP40). RIPA buffer-equilibrated FLAG Affinity M2Ab Resin (10 μ l; Kodak, Sigma) was then added and the sample was rotated for 1.5 hr at 4°C. The resin was pelleted and washed three times with 1 ml cold RIPA buffer. Proteins were eluted by boiling in 30 μ l 2 \times sample loading buffer and were separated by 12% SDS PAGE. Immunoblot analysis was performed with antibodies directed against the N-terminal 79 amino acids of Ikaros (Hahm et al., 1994, 1998). Goat α -rabbit Ig (Zymed) was used as secondary antibody. ECL (Amersham) was used for visualization.

Chemical Crosslinking

Cytoplasmic lysates (10 μ l, 40 μ g) were adjusted to 50 μ l with buffer H₆₀. Disuccinimidyl suberate (DSS) dissolved in DMSO (5 mg/ml) was added at final concentrations ranging from 0.1 to 2 μ g/ μ l. Crosslinking reactions were carried out at room temperature and were stopped by the addition of an equal volume of 2 \times sample loading buffer. Crosslinked products were separated by SDS-PAGE, followed by immunoblot analysis.

Homology Modeling

The Ikaros DZF sequence was used to search the Protein Data Bank (PDB) for similar sequences. The zinc fingers of a TATA box binding protein, PDB code 1G2D (Wolfe et al., 2001), share 30% sequence identity with both fingers of the Ikaros DZF. The cysteine and histidine residues allowed accurate alignment of the DZF and TATA box binding protein sequences. In addition, the zinc-finger domains of the human enhancer binding protein, MBP-1 (PDB code 1BBO [Omichinski et al., 1992]), share 23% sequence identity with the DZF sequence. Like the Ikaros DZF, the C-terminal finger of MBP-1 has an atypical 5 residue spacer between histidine residues, which provided additional information for the modeling of the DZF structure.

Homology modeling was accomplished using the program MODELLER6v2, which uses spatial restraints derived from the alignments to arrive at the most probable structure for a sequence (Sali and Blundell, 1993). One advantage of this program is that multiple alignments to the target sequence may be used. The Ikaros DZF homology model was generated and manually inspected for steric clashes between residues.

Acknowledgments

We thank James Bowie and Michael Haykinson for helpful advice and critical reading of the manuscript. This work was supported by P.H.S. Training Grant CA009120 to A.S.M. D.E. and S.T.S. are Investigators of the Howard Hughes Medical Institute.

Received: July 26, 2002

Revised: November 22, 2002

References

- Ausubel, F.M. (1995). *Short Protocols in Molecular Biology*, Third Edition (New York: John Wiley and Sons Ltd.).
- Bellon, S.F., Rodgers, K.K., Schatz, D.G., Coleman, J.E., and Steitz, T.A. (1997). Crystal structure of the RAG1 dimerization domain reveals multiple zinc-binding motifs including a novel zinc binuclear cluster. *Nat. Struct. Biol.* 4, 586–591.
- Brown, K.E., Guest, S.S., Smale, S.T., Hahm, K., Merckenschlager, M., and Fisher, A.G. (1997). Association of transcriptionally silent genes with Ikaros complexes at centromeric heterochromatin. *Cell* 91, 845–854.
- Brown, K.E., Baxter, J., Graf, D., Merckenschlager, M., and Fisher, A.G. (1999). Dynamic repositioning of genes in the nucleus of lymphocytes preparing for cell division. *Mol. Cell* 3, 207–217.
- Cobb, B.S., Morales-Alcelay, S., Kleiger, G., Brown, K.E., Fisher, A.G., and Smale, S.T. (2000). Targeting of Ikaros to pericentromeric heterochromatin by direct DNA binding. *Genes Dev.* 14, 2146–2160.
- Ernst, P., Hahm, K., Cobb, B.S., Brown, K.E., Trinh, L.A., McCarty, A.S., Merckenschlager, M., Klug, C.A., Fisher, A.G., and Smale, S.T. (1999). Mechanisms of transcriptional regulation in lymphocyte progenitors: insight from an analysis of the terminal transferase promoter. *Cold Spring Harb. Symp. Quant. Biol.* 64, 87–97.
- Fox, A.H., Kowalski, K., King, G.F., Mackay, J.P., and Crossley, M. (1998). Key residues characteristic of GATA N-fingers are recognized by FOG. *J. Biol. Chem.* 273, 33595–33603.
- Georgopoulos, K. (2002). Haematopoietic cell-fate decisions, chromatin regulation and Ikaros. *Nature Rev. Immunol.* 2, 162–174.
- Hahm, K., Ernst, P., Lo, K., Kim, G.S., Turck, C., and Smale, S.T. (1994). The lymphoid transcription factor LyF-1 is encoded by specific, alternatively spliced mRNAs derived from the Ikaros gene. *Mol. Cell. Biol.* 14, 7111–7123.
- Hahm, K., Cobb, B.S., McCarty, A.S., Brown, K.E., Klug, C.A., Lee, R., Akashi, K., Weissman, I.L., Fisher, A.G., and Smale, S.T. (1998). Helios, a T cell-restricted Ikaros family member that quantitatively associates with Ikaros at centromeric heterochromatin. *Genes Dev.* 12, 782–796.
- Honma, Y., Kiyosawa, H., Mori, T., Oguri, A., Nikaido, T., Kanazawa, K., Tojo, M., Takeda, J., Tanno, Y., Yokoyama, S., et al. (1999). Eos: a novel member of the Ikaros gene family expressed predominantly in the developing nervous system. *FEBS Lett.* 447, 76–80.
- Horton, R.M. (1995). PCR-mediated recombination and mutagenesis. SOEing together tailor-made genes. *Mol. Biotechnol.* 3, 93–99.
- Isalan, M., Klug, A., and Choo, Y. (2001). A rapid, generally applicable method to engineer zinc fingers illustrated by targeting the HIV-1 promoter. *Nat. Biotechnol.* 19, 656–660.
- Klemm, J.D., Schreiber, S.L., and Crabtree, G.R. (1998). Dimerization as a regulatory mechanism in signal transduction. *Annu. Rev. Immunol.* 16, 569–592.
- Lander, E.S., Linton, L.M., Birren, B., Nusbaum, C., Zody, M.C., Baldwin, J., Devon, K., Dewar, K., Doyle, M., FitzHugh, W., et al. (2001). Initial sequencing and analysis of the human genome. *Nature* 409, 860–921.
- Lee, J.S., Galvin, K.M., and Shi, Y. (1993). Evidence for physical interaction between the zinc-finger transcription factors YY1 and Sp1. *Proc. Natl. Acad. Sci. USA* 90, 6145–6149.
- Liew, C.K., Kowalski, K., Fox, A.H., Newton, A., Sharpe, B.K., Crossley, M., and Mackay, J.P. (2000). Solution structures of two CCHC zinc fingers from the FOG family protein U-shaped that mediate protein-protein interactions. *Struct. Fold. Des.* 8, 1157–1166.
- Mackay, J.P., and Crossley, M. (1998). Zinc fingers are sticking together. *Trends Biochem. Sci.* 23, 1–4.
- Miller, J., McLachlan, A.D., and Klug, A. (1985). Repetitive zinc-binding domains in the protein transcription factor IIIA from *Xenopus oocytes*. *EMBO J.* 4, 1609–1614.
- Molnar, A., and Georgopoulos, K. (1994). The Ikaros gene encodes a family of functionally diverse zinc finger DNA-binding proteins. *Mol. Cell. Biol.* 14, 8292–8303.
- Momeni, P., Glockner, G., Schmidt, O., von Holtum, D., Albrecht, B., Gillissen-Kaesbach, G., Hennekam, R., Meinecke, P., Zabel, B., Rosenthal, A., et al. (2000). Mutations in a new gene, encoding a zinc-finger protein, cause tricho-rhino-phalangeal syndrome type I. *Nat. Genet.* 24, 71–74.
- Omichinski, J.G., Clore, G.M., Robien, M., Sakaguchi, K., Appella, E., and Gronenborn, A.M. (1992). High-resolution solution structure of the double Cys2His2 zinc finger from the human enhancer binding protein MBP-1. *Biochemistry* 31, 3907–3917.
- O’Shea, E.K., Rutkowski, R., and Kim, P.S. (1992). Mechanism of specificity in the Fos-Jun oncoprotein heterodimer. *Cell* 68, 699–708.
- Pabo, C.O., Peisach, E., and Grant, R.A. (2001). Design and selection of novel Cys2His2 zinc finger proteins. *Annu. Rev. Biochem.* 70, 313–340.
- Payre, F., Buono, P., Vanzo, N., and Vincent, A. (1997). Two types of zinc fingers are required for dimerization of the serendipity delta transcriptional activator. *Mol. Cell. Biol.* 17, 3137–3145.
- Perdomo, J., Holmes, M., Chong, B., and Crossley, M. (2000). Eos and pegasus, two members of the Ikaros family of proteins with distinct DNA binding activities. *J. Biol. Chem.* 275, 38347–38354.
- Sali, A., and Blundell, T.L. (1993). Comparative protein modelling by satisfaction of spatial restraints. *J. Mol. Biol.* 234, 779–815.
- Schwabe, J.W., and Klug, A. (1994). Zinc mining for protein domains. *Nat. Struct. Biol.* 1, 345–349.
- Segal, D.J., and Barbas, C.F., 3rd. (2000). Design of novel sequence-specific DNA-binding proteins. *Curr. Opin. Chem. Biol.* 4, 34–39.
- Segal, D.J., and Barbas, C.F., 3rd. (2001). Custom DNA-binding proteins come of age: polydactyl zinc-finger proteins. *Curr. Opin. Biotechnol.* 12, 632–637.
- Sellers, J.W., and Struhl, K. (1989). Changing fos oncoprotein to a jun-independent DNA binding protein with GCN4 dimerization specificity by swapping “leucine zippers”. *Nature* 341, 74–76.
- Sun, L., Liu, A., and Georgopoulos, K. (1996). Zinc finger-mediated protein interactions modulate Ikaros activity, a molecular control of lymphocyte development. *EMBO J.* 15, 5358–5369.
- Tautz, D., Lehmann, R., Schnuerch, H., Schuh, R., Seifert, E., Kienlin, A., Jones, K., and Jaecle, H. (1987). Finger protein of novel structure encoded by hunchback, a second member of the gap class of *Drosophila* segmentation genes. *Nature (Lond.)* 327, 383–389.
- Trinh, L.A., Ferrini, R., Cobb, B.S., Weinmann, A.S., Hahm, K., Ernst, P., Garraway, I.P., Merckenschlager, M., and Smale, S.T. (2001). Down-regulation of TDT transcription in CD4(+)CD8(+) thymocytes by Ikaros proteins in direct competition with an Ets activator. *Genes Dev.* 15, 1817–1832.
- Venter, J.C., Adams, M.D., Myers, E.W., Li, P.W., Mural, R.J., Sutton, G.G., Smith, H.O., Yandell, M., Evans, C.A., Holt, R.A., et al. (2001). The sequence of the human genome. *Science* 291, 1304–1351.
- Wolfe, S.A., Nekludova, L., and Pabo, C.O. (2000). DNA recognition by Cys2His2 zinc finger proteins. *Annu. Rev. Biophys. Biomol. Struct.* 29, 183–212.
- Wolfe, S.A., Grant, R.A., Elrod-Erickson, M., and Pabo, C.O. (2001). Beyond the “recognition code”: structures of two Cys2His2 zinc finger/TATA box complexes. *Structure (Camb)* 9, 717–723.
- Wuttke, D.S., Foster, M.P., Case, D.A., Gottesfeld, J.M., and Wright, P.E. (1997). Solution structure of the first three zinc fingers of TFIIIA bound to the cognate DNA sequence: determinants of affinity and sequence specificity. *J. Mol. Biol.* 273, 183–206.
- Zhou, Q., Gedrich, R.W., and Engel, D.A. (1995). Transcriptional repression of the c-fos gene by YY1 is mediated by a direct interaction with ATF/CREB. *J. Virol.* 69, 4323–4330.